IEEE Access
Multidisciplinary | Rapid Review | Open Access Journal

Received March 4, 2019, accepted March 14, 2019, date of publication March 20, 2019, date of current version April 10, 2019.

Digital Object Identifier 10.1109/ACCESS.2019.2906269

A Multi-Objective Allocation Approach for Power Quality Monitoring Devices

MOSTAFA F. SHAABAN, (Member, IEEE), AHMED H. OSMAN, (Senior Member, IEEE), AND FATEMA M. ASEERI

Electrical Engineering Department, American University of Sharjah, Sharjah, UAE

Corresponding author: Mostafa F. Shaaban (mshaaban@aus.edu)

This work was supported by the American University of Sharjah under Grant FRG17-R-41.

ABSTRACT With the inception of smart grids and the increased integration of renewable resources, the continuous monitoring of power systems becomes increasingly important to monitor power quality (PQ) and speed up the localization of faults. The optimal allocation of PQ monitoring devices to achieve 100% observability is one of the most important design problems that face the planning of any power system. However, for smart distribution networks (SDNs), the cost of achieving 100% observability is exorbitant. Therefore, for cost-effective monitoring, the SDN planers can sacrifice a percentage of the system observability. To that end, this paper proposes a multi-objective optimization approach for allocating the PQ monitoring devices with the aim of minimizing two conflicting objectives, namely, the cost and the loss of observability in the system. The proposed approach utilizes branch-and-reduce-based nonlinear programming global solver that minimizes both objectives. The analysis is first carried out for balanced systems and later extended to unbalanced systems. To validate the performance of the proposed approach, it is applied to different standard systems. The obtained results prove the effectiveness of the proposed approach.

INDEX TERMS Multi-objective optimization, power quality monitoring, system observability.

I. INTRODUCTION

Monitoring of the distribution network status is of utmost importance to enhance the system reliability, increase customer's satisfaction, and minimize the operating cost. Grid operators aim to monitor the status of the distribution system by installing supervisory control and data acquisition (SCADA) units. Due to financial limitations, they do not monitor every node or customer; rather they install few SCADA units to monitor specific nodes in the system. In practice, only 3-5% of the total number of nodes in the distribution system are monitored. For conventional distribution networks, this percentage is sufficient to give the operators in the substations a good idea about the system status as of voltage levels, current flows, and power flows [1], [2]. However, in order to perform adequate management under the umbrella of smart grids, higher and more precise observability is required compared to conventional distribution networks.

More recently, utilities are implementing demand response programs and are encouraging customers to install renewable distributed generation. However, integrating renewable resources in these systems is expected to cause power quality (PQ) problems due to their intermittent nature and the fact that these systems were not originally designed to accommodate such generation. Thus, the power quality indices have to be monitored at all times to ensure adequate supply and customer satisfaction. However, the traditional metering devices are not useful as they only provide magnitudes of voltages, currents and powers every few minutes. On the other hand, power quality devices such as phase measurement units (PMUs) can measure synchronized state variables. Therefore, the observability of the system states (voltages and currents) can be used to calculate PQ indices [3].

While many power transmission systems aim at achieving 100% observability of the system, the same requirement is not present for most smart distribution networks (SDNs) where a certain degree of loss in system observability can be tolerated at the expense of a large reduction in the cost.

The objective of the work at hand is to optimize the number and locations of monitoring equipment installed in an SDN with respect to the total cost of the equipment and the achieved degree of observability. To that end, this work proposes a multi-objective optimal allocation approach for monitoring devices in the SDNs. The two objectives considered

The associate editor coordinating the review of this manuscript and approving it for publication was Guido Carpinelli.

in the work are the cost of the monitoring equipment and the loss of observability in monitoring the system variables. To optimize both objective functions jointly, an exact deterministic solver is used to generate the set of Pareto optimal solutions. To address practical distribution networks, the proposed approach is developed for balanced networks and later extended to unbalanced networks.

The contributions of this work can be summarized as follows:

- Developing a new formulation for the observability in unbalanced networks.
- Proposing a new multi-objective approach considering monitoring devices allocation with weighted regions.
- Comparing different solution approaches, namely the exact solvers to metaheuristic solvers.

The rest of this paper is organized as follows. An overview of the related work is presented in section II. The system observability is discussed and formulated in Section III. The details of the cost breakdown of the monitoring equipment are discussed in Section IV. The multi-objective optimization formulation is discussed in Section V. Case studies and simulation results are presented in Section VI. The paper is finally concluded in Section VII.

II. RELATED WORK

There have been multiple approaches taken in the literature with regards to the monitoring devices allocation problem [2]–[13]. Most of the previous work models the problem as a mathematical optimization problem that is solved using different techniques including integer linear programming, particle swarm optimization, and genetic algorithms.

Martins *et al.* [2] approached the allocation problem from a fault location perspective and aim at placing the monitoring devices in locations that are closest to the disturbance sources. In this regard, a unique identification of the locations of these disturbances is maximized, while simultaneously aiming at reducing the cost. These two objectives are optimized using a multi-objective optimization problem that is solved using the Bicriteria Discrete Optimization algorithm.

de Freitas *et al.* [4] presented a case study in which they proposed a method to allocate the monitoring devices such that the total cost is reduced while guaranteeing 100% observability. They do so by formulating the problem as a binary integer-programming problem that can be solved by the Branch and Bound Method. The final solution from the set of optimal solutions obtained is chosen using a data redundancy factor metric, which defines the average number of times a state is observed for certain location placement of the monitoring equipment.

Martins *et al.* [5] proposed the use of Clonal Selection Algorithm to solve the monitoring devices allocation problem. The objective is to find the minimum number of monitoring equipment that would guarantee complete monitoring of all short-circuit conditions in the system. The algorithm takes into account the presence of symmetries in the system, which further complicates the identification of fault conditions.

Silva *et al.* [6] proposed an allocation scheme that focuses on the importance and relative distance of the loads especially in systems where nontechnical losses are the main reason for voltage sags. They apply the P-Median model as a second step after obtaining the optimal locations of the monitors to have complete observability in the system. The final allocation of the monitoring equipment is obtained by using the P-Median algorithm. Locations of the monitoring equipment are prioritized based on the importance of the load.

Oleskovicz *et al.* [7] formulated the allocation problem as a nonlinear integer-programming problem with the objective of minimizing the total cost while simultaneously maximizing the redundancy of measurements. The problem formulation considers mainly the main circuit topology without considering the load parameters and is solved using a Compact Genetic Algorithm structure, which reduces the computational complexity of the solution. Branco *et al.* [8] exploited the linkage learning in Extended Compact Genetic Algorithm to solve the same problem scaled to large systems with large number of buses and interconnections.

Cebrian *et al.* [9] proposed an allocation scheme that aims at finding the minimum number of location of the monitoring equipment to maximize a detection capability index. The problem formulation is based on characterizing the system in terms of the most likely short circuits that could occur in the system. The authors proposed a method that considers different combinations of variables such as the fault location, fault type, and fault impedance to simulate several short circuits at different points in the system and select the most relevant ones to be considered.

Almeida and Kagan [10] developed an allocation problem formulation based on the characterization of the system behavior in terms of voltage variations during different types of short circuits at different points in the system. To solve the problem, they employ Genetic Algorithms and Fuzzy Set Programming.

Reis *et al.* [11] followed a different approach by considering a single objective optimization formulation that aims at reducing the total cost of the monitoring equipment. The observability requirements are then added as a set of constraints to the problem. The formulation of the constraints only considers the circuit topology without requiring the knowledge about the load or generation at the system buses.

Kempner *et al.* [12] proposed a method to determine the largest vulnerability area around each bus by constructing voltage sags matrices for each short circuit type using the Fault Positions Method. The monitoring allocation problem is formulated as an integer linear programming problem to find the minimum number and locations of the monitoring equipment that would maximize the covered vulnerability area.

Dai *et al.* [13] employed particle swarm optimization in solving the monitoring allocation optimization problem. The problem is modeled using an integer programming model. The objective is to minimize the number of monitoring equipment subject to the constraint of capturing each fault

position a certain number of times in the covered ranges of the monitoring equipment. Eldery *et al.* [14] introduced a novel approach for allocating monitoring devices, in which they utilized a deterministic solver for the integer programming problem. However, this approach is only suitable for balanced systems.

While all the works cited above aim to achieve 100% observability of the system, this work aims to find the optimal compromise between observability and cost. We do so by finding the set of Pareto optimal solutions that minimize both the cost and the loss of the observability in the system. This enables the cost-benefit analysis of several equally optimal solutions. The final decision of choosing one of the provided optimal solutions is entirely up to the planning entity of the distribution system. Moreover, all the above works focus on balanced systems, while in practice, most distribution systems are unbalanced. Consequently, the proposed approach is extended to cover unbalanced systems.

III. SYSTEM OBSERVABILITY

Depending on the location of placement of the monitoring equipment, various degrees of system observability can be achieved. Hence, given a certain budget for installing monitoring devices, finding their optimal placement location such that the total system observability is maximized, is one of the greatest challenges facing the system designer. In the formulation and henceforth, observability is defined as the percentage of the states that can be fully observed in the system for a certain location combination of the monitoring devices, viz,

$$Obs = \frac{\sum_{s=1}^{M} O_s}{M} \times 100\%, \tag{1}$$

where $\mathbb{S}$ is the set of all possible observable states $S = \{1, 2, \ldots, M\}$, M is the total number of observable states, s is the index of states $s \in \mathbb{S}$, and O_s is the binary observability vector, which indicates whether each state s is observable or not using the current location combination.

For a balanced 3-phase system, the observable state variables consist of the voltage at each bus and the current in the lines between the buses. Hence, the total number of observable state variables can be calculated from the connectivity of the system using the connection parameter of the system in the following manner. Let $\mathbb{S}^V, \mathbb{S}^I \subset \mathbb{S}$ denotes the subset of voltage states and the subset of current states. Let M^V and M^I denote the number of voltage and current observable state variables, respectively. Let N denotes the total number of buses in the system and $D_{i,j}$ denotes the connection parameter, which is a binary parameter. Assume $i \in \mathbb{J}$ and $j \in \mathbb{J}$ to be the bus indices and $\mathbb{J}$ to be the set of buses, where $\mathbb{J} = \{1, 2, \ldots, N\}$ for an N-bus system. Then, any parameter $D_{i,j}$ is 1 for $i = j$. And for $i \neq j$, $D_{i,j} = 1$ if there is a connection between buses i and j, and 0 otherwise.

To calculate the total number of observable states M from the connection parameter D, we add the number of voltage states of the buses M^V to the number of current states M^I as in (2). The total number of voltage states M^V is the sum of $D_{i,j}$ $\forall i = j$, which is simply the number of buses N. The number of current states M^I can be calculated by adding the connection parameter and subtracting the self elements N, and dividing by 2 to extract only one current state between any two buses, as illustrated in (2).

$$\left.\begin{aligned} M^V &= N \\ M^I &= \frac{\sum_{i=1}^{N}\sum_{j=1}^{N} D_{i,j} - N}{2} \\ M &= M^V + M^I \end{aligned}\right\} \tag{2}$$

For an unbalanced system, where each bus may not have all three phases connected, the problem can be reformulated as such.

Unlike the balanced system case, the phase voltages at each bus and the phase currents in the lines connected to the bus are considered as separate states. Hence, each bus will have up to 3 voltage states, and every two connected buses will have up to 3 observable current states. For generality, we redefine the connection parameter as $D^{UNB}_{i,j,p}$ for unbalanced systems, where p are the phase index and $\mathbb{P}$ is the set of phases, respectively, i.e. $p \in \mathbb{P} = \{1, 2, 3\}$. The three elements $D^{UNB}_{i,j,p}$ $\forall i = j$ for any bus i in an unbalanced systems do not have to be all ones like balanced systems since some buses may not have all the three phases. Therefore, to find the number of voltage states M^V, we add the connection parameter for all $i = j$, as shown in (3). To calculate the number of the current states M^I, we find the difference between the sum of all connection parameter elements and M^V, and then we divide the outcome by 2, as in (2). Finally, the total number of observable states M for an unbalanced system of N buses given the connection parameter $D^{UNB}_{i,j,p}$ can be calculated as in (3).

$$\left.\begin{aligned} M^V &= \sum_{i\in\mathbb{J}}\sum_{p\in\mathbb{P}} D^{UNB}_{i,j,p} \\ M^I &= 0.5 \times \left(\left(\sum_{i\in\mathbb{J}}\sum_{j\in\mathbb{J}}\sum_{p\in\mathbb{P}} D^{UNB}_{i,j,p}\right) - M^V\right) \\ M &= M^V + M^I \end{aligned}\right\} \tag{3}$$

By placing the monitoring equipment in a certain combination of locations, each state may be observable more than once by multiple monitoring equipment simultaneously. Hence, to determine the observability of each state in the system, multiple approaches such as Ohm's Law and Kirchhoff's Current Law (KCL) can be taken to find the relationships between the nodes.

Three types of vectors can be used to determine the observability of each state in the system as defined in [14]. These are the observability vector O_s^{CN1}, the co-observability vector O_s^{CN2}, and the KCL co-observability vector O_s^{CN3}. These vectors are constructed using two types of parameters, the Connectivity parameter $A_{s,i}$, and the Co-Connectivity parameter $B_{s,i}$. These binary parameters determine the observability of each state s by placing a monitoring device on bus i and leveraging Ohm's law and KCL.

According to [14] the connectivity parameter $A_{s,i}$ of a system can be constructed leveraging Ohm's law that relates

the voltages at two connected nodes to the current passing between them. As a result, if the voltage and current at a certain bus are observable, the voltage at the other buses connected to this bus are observable too. Additionally, if the voltages at two buses are observable, the current flowing between them is observable too.

Applying the same idea, the co-connectivity parameter $B_{s,i}$ is constructed for the currents in the system that are not directly observable by the monitoring equipment at each node. For example, if any two buses i and j are connected to two other buses $i-1$ and $j+1$ that have monitoring equipment installed on them, the current $I_{i,j}$ between buses i and j can be indirectly calculated using the values of the voltages V_i and V_j that can be calculated using the directly observable voltages and currents at buses $i-1$ and $j+1$. Hence, each system will have two co-connectivity parameters $B_{s,i}^{CC1}$ and $B_{s,i}^{CC2}$ indicating the potential of each current state s being observable from each location i. A current state is deemed observable if the same entry in both parameters equals to 1. The observability and co-observability vectors are calculated by multiplying these parameters with the location vector X_i. The binary location vector X_i is 1 if a monitoring device is located at bus i, and 0 otherwise, i.e.

$$X_i = \begin{cases} 1, & \textit{if a monitor is installed at bus } i \\ 0, & \textit{otherwise} \end{cases} \tag{4}$$

A third type of observability vector, denoted the KCL co-observability vector, is calculated with the known load parameters. Leveraging the lemma that if the voltages of all the buses connected to a known load bus are observable, the voltage of this bus is observable as well, the observability of the buses with the known loads can be determined.

Hence, by combining all the Observability and Co-Observability vectors, and projecting the location vector X onto them, the number of times each state in the system is observable can be accurately determined.

For the unbalanced 3-phase systems, the same connectivity and Co-connectivity parameters can be utilized with some modifications. As mentioned earlier, for an unbalanced system, each phase of each bus contributes a different voltage and current state. In addition, due to the absence of some phase connections in certain buses, installing a monitoring device on a single bus can result in a different degree of observability contribution from one bus to another.

The objective of the problem is to find the optimal placement of the monitoring equipment of the buses of the system. Hence, the $A_{s,i}, B_{s,i}^{CC1}$ and $B_{s,i}^{CC2}$ parameters are going to retain the bus index i which indicate the location of installation of the monitoring equipment in terms of the system buses. The second index, however, will be changed to indicate the new system states. Each state s will represent a single-phase voltage for the first M^V states and a single-phase current for the remaining M^I states. In the case where a connection does not exist to a certain phase in the bus, the corresponding state s is omitted. The details of the construction of these parameters are shown in Fig. 1 and are outlined in Algorithm 1 in Appendix A.

Finally, the observability vector O_s can be determined as follows:

$$\left.\begin{aligned} O_s^{CN1} &= A_{s,i} \times X_i \\ O_s^{CN2} &= B_{s,i}^{CC1} \times X_i \\ O_s^{CN3} &= B_{s,i}^{CC2} \times X_i \\ O_s^{Mult} &= O_s^{CN1} + (O_s^{CN2} \odot O_s^{CN3}) \\ O_s &= \min(O_s^{Mult}, 1) \end{aligned}\right\} \tag{5}$$

As in (5), a state can be observable from the simple observability vector O_s^{CN1} or from the co-observability vectors O_s^{CN2} and O_s^{CN3}. However, for the co-observability vectors, for a state to be observable, its entry in both vectors must be 1, as shown in the multiplication in (5). The multi-observability vector O_s^{Mult} reflects how many times each state s is observed by the allocated monitoring devices. For any value more than 1, the binary observability vector is set to 1, as given in (5).

IV. COST FUNCTION

The cost of the monitoring equipment is defined as the summation of two quantities, a fixed cost and a variable cost. The fixed cost includes the installation cost in addition to the basic cost of the equipment. The variable cost increases based on the number of transducers included in the monitoring equipment and hence is dependent on the number of connections in each bus and consequently the location of the bus. To calculate the variable cost, we first find the number of connections at each bus. This can be represented by the vector n_i, which represents the number of lines connected to each bus. To construct n_i, we use the connection parameter D as in (6) for a balanced three phase system, where all the connections between bus i to other buses are added.

For unbalanced systems, the same can be applied by summing all phases' lines connected between any two buses i, j such that $j \neq i$, as in (7).

$$n_i = \sum_{j \neq i}^{N} D_{i,j}, \quad \forall i \in \mathbb{J} \tag{6}$$

$$n_i = \sum_{j \neq i}^{N} \sum_{p \in \mathbb{P}} D_{i,j,p}^{UNB}, \quad \forall i \in \mathbb{J} \tag{7}$$

Hence, the cost C_i of installing an equipment at bus i is calculated as

$$C_i = c^{fix} + c^{var} \times n_i, \quad \forall i \in \mathbb{J} \tag{8}$$

where c^{fix} and c^{var} represent the fixed and variable costs for installing a monitoring device, respectively.

V. PROBLEM FORMULATION

So far, two conflicting objectives are defined in the problem formulation. These are the total cost of the monitoring equipment and the total loss of observability of the system. The objective of the proposed algorithm is to find the optimal

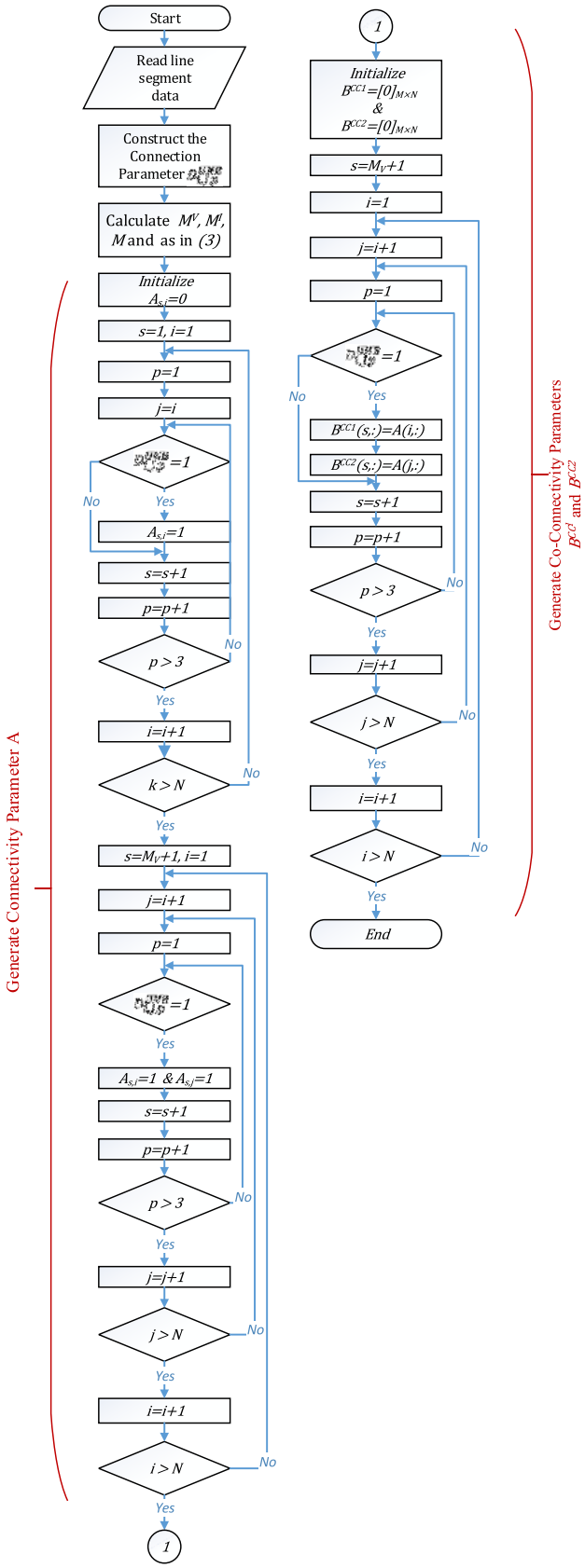

FIGURE 1. The procedure to generate the connectivity and co-connectivity parameters for unbalanced networks.

number and placement of the monitoring equipment such that these two objectives are minimized.

However, naturally, reducing one objective would lead to an increase in the other. In order to reduce the cost by reducing the number of monitoring equipment in the system, certain states in the system might not be observable thus leading to an increase in the loss of observability. The opposite holds true as well. In order to ensure that all the states in the system are observable, a large number of monitoring devices may be needed which will increase the cost. To find the exact relationship between these two variables for any system, we propose the use of an optimization framework that would enable us to generate the set of Pareto optimal solutions to better examine the cost-benefit analysis of several optimal solutions and better inform the decision making process. To that end, we formulate the problem as a multi-objective optimization problem with the two objective functions, $f1$ and $f2$, denoting the total cost and the loss of observability in the system, respectively.

We first define the binary location vector X in (4) to be the decision variable of the allocation problem. The objective is then to find the optimal location vector X that would minimize both the cost and the loss of the system observability. The monitoring devices allocation problem is defined as Mixed Integer Nonlinear Programming (MINLP) and is formulated as in (9).

$$\left.\begin{aligned} &\min_{X} (f_1, f_2) \\ &f_1 = \sum_{i\in\mathbb{J}} C_i \times X_i \\ &f_2 = \left(1 - \frac{\sum_{s\in\mathbb{S}} O_s}{M}\right) \times 100\% \\ &S.T.\,(4,5) \\ &x_i \in \{0,1\} \quad \forall x_i \in X \end{aligned}\right\} \tag{9}$$

VI. MULTI-OBJECTIVE OPTIMIZATION

To solve the multi-objective allocation problem, there are several approaches proposed in the literature. Peng *et al.* [15] and Shaaban and El-Saadany [16] proposed the use of the Genetic Algorithms, specifically, the non-dominating sorting genetic algorithm (NDSGA). In other works, Liu *et al.* [17] and Baghaee *et al.* [18] utilized multi-objective particle swarm optimization (PSO). However, despite that the solution provided by these meta-heuristic techniques is very close to the true Pareto-optimal front, satisfactory in most cases, and has fast computational time, there is no guarantee or a measure of how close is the solution to the true Pareto-Optimal front.

Therefore, in the proposed algorithm we employ the branch-and-reduce optimization navigator (BARON) [19], which relies on branch-and-reduce algorithm combined with a nonlinear programming solver, such as internal point optimization (IPOPT). The BARON guarantees the optimality of the solution for the MINLP proposed problem within a specified tolerance of 10^{-6}. However, the BARON solver is not tailored to be used for multi-objective optimization.

TABLE 1. Number of states for each system.

System	M^V	M^I	M
6-bus [14]	6	8	14
30-bus [14]	30	41	71
38-bus [20]	38	37	75
123-bus [21]	253	247	500

Thus, we propose the use of the constraint method to generate the true Pareto Front. This is performed by converting one of the objectives into a constraint and solving multiple problems with different bounds on this constraint. Hence, the allocation problem in (9) is solved as follows:

- Step 1: Solve the allocation problem in (9) to minimize only the cost objective while setting a constraint of 0 % loss of observability, i.e. $f_2 = 0\%$. Denote the minimum cost to gain 0 % loss of observability as f_1^{MIN}.
- Step 2: Resolve the allocation problem in (9) to minimize only the loss of observability objective while setting a constraint to limit the cost as $f_1 \leq C^{MAX}$.
- Step 3: Repeat step 2 for increments in the cost as $C^{MAX} = 0 : \delta : f_1^{MIN}$, where δ is the cost step and should be chosen to match integer multiples of c^{fix} and c^{var}. There is no need to have a very small step as the cost of allocation only varies as integer multiples of c^{fix} and c^{var}, as seen in (8).

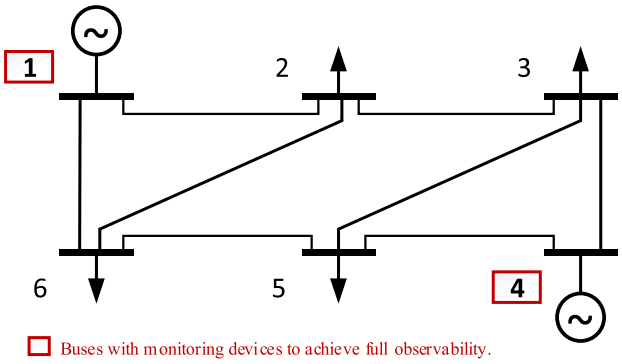

FIGURE 2. The balanced 6-bus system [14].

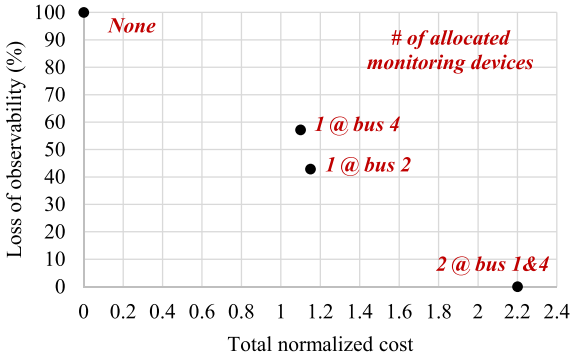

FIGURE 3. The Pareto front results for the 6-bus system.

VII. CASE STUDIES AND VALIDATION

In this section, we validate the performance of the proposed algorithm by applying it to different case studies. Specifically, we test the algorithm with four different systems ranging in size and in structure. The four case studies are introduced to highlight the difference between meshed power systems versus distribution radial systems and balanced versus unbalanced systems. The first two case studies present meshed transmission systems, while the last two case studies present radial distribution feeders. For the meshed systems, we choose the balanced meshed 6-bus system and the standard IEEE 30-bus system in [14]. For radial distribution systems, we choose the 38-bus system in [20] and the IEEE 123-bus test feeder [21]. The IEEE 123-bus test feeder is also selected for being an unbalanced system, which tests the versatility and the generalizability of our algorithm to different types of systems. The numbers of states for the systems under study are shown in Table 1.

For all the four systems, we generate the set of Pareto optimal solutions using our algorithm and plot the generated Pareto front. The next four sections provide more details for each of the four cases.

A. THE BALANCED 6-BUS SYSTEM

We first test the algorithm with a balanced small-scale meshed three phase power system represented by the 6-bus system shown in Fig.2. The generated Pareto front for the system is shown in Fig.3. It can be noted that the Pareto front is quite sparse and that is due to the small number of decision variables in the problem (6 in this case). Due to the small size of this system, the complete Pareto front results are shown in Fig. 3. The trend in the graph is as expected. The loss of system observability reduces drastically with the increase in the total cost. The total cost is represented as the normalized cost with respect to the fixed cost. In other words, for each individual monitoring equipment, the fixed cost is normalized to a value of 1.0. Then, depending on the number of lines connected to each bus, a variable cost of 5% of the fixed cost is added to the total cost, i.e. the cost step δ is chosen to be 5%.

Examining the set of optimal solutions more carefully, we find that the optimal number of monitoring equipment does not exceed 2 for the best-case scenarios (on buses 1 and 4), as shown in Fig. 2, which is enough to have any bus in the system either with a monitoring device or connected to a bus with a monitoring device. This result is the same result as in [14]. However, in [14], the focus was to minimize redundancy in measured values, not the cost. For the results to be matching, it is a coincidence that for this small system the allocation for 100 % observability and minimum redundancy is the same for minimum cost.

The performance of the system in terms of the loss of observability depends on the location of the monitoring equipment. The number of monitoring equipment can be, however, reduced to 1 at the expense of suffering, at best,

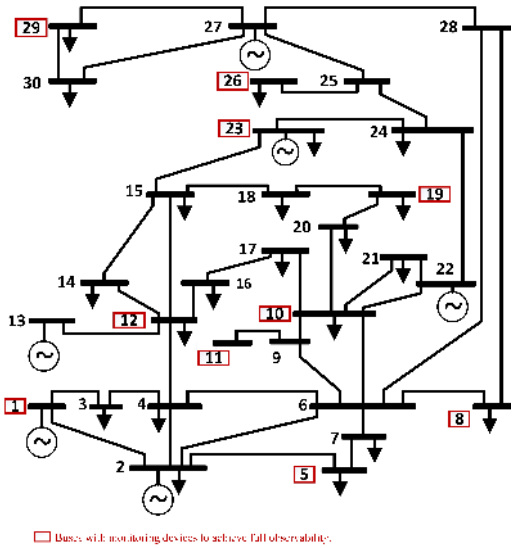

FIGURE 4. The balanced IEEE 30-bus system [14].

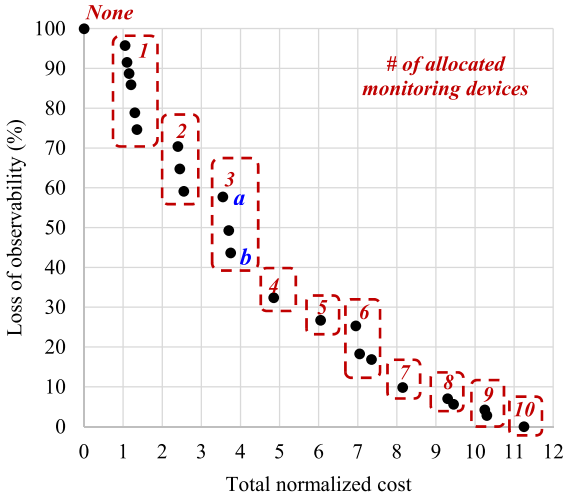

FIGURE 5. The Pareto front results for the IEEE 30-bus system.

around 42.86 % loss of observability. This indicates that the proposed algorithm does indeed provide the best tradeoff between cost and observability, giving the planning entity a multitude of options to choose from. Also, as shown in Fig. 3, if one monitoring device is placed at bus 4, a cost of 1.10 would result in observability loss of about 57.14 %. However, a slightly higher cost of 1.15 is required to place a monitoring device on bus 2 to reduce the loss of observability to 42.86 %.

B. THE BALANCED 30-BUS SYSTEM

In this case study, the proposed algorithm is applied to the balanced meshed IEEE 30-bus system shown in Fig. 4. The generated Pareto front is shown in Fig. 5. As shown, the Pareto front in this case is more densely populated than the 6-bus case. This is attributed to the larger number of decision variables to be solved for in the problem. The same trend is observed again, confirming the expected tradeoff between cost and system observability.

Examining the graph more closely we find that, even though the total number of buses in the system is 30, a number of monitoring devices as few as 7 is enough to limit the loss of observability in the system to just below 10%. On the other hand, to achieve 100% observability of the system, only 10 monitoring devices located as shown in Fig. 4 are needed, which coincide with the results presented in [14]. It can also be noted that the variation in the cost appears in groups, where each group represents a certain number of allocated monitoring devices and the variation in the cost is related to the transducers cost. Fig. 5 indicates that from one optimal solution to another, changing the configuration of the monitoring equipment by adding an extra one contributes greatly to reducing the observability loss. Moreover, it can be observed in Fig. 5 that for each number of allocated monitoring devices, there is a band of observability that can be achieved by changing the optimal location of these devices with slight variation in cost. It is noted that with a fewer number of monitoring devices, the band of observability is wide and decreases as the number of allocated devices increases. For example, allocating 3 monitoring devices on buses 12, 22, and 28 with a cost of 3.55 results in loss of observability of 57.75% as shown for the solution "a" in Fig. 5. Reallocating these monitoring devices to buses 6, 12, and 25 results in loss of observability of 43.66% only with an increase in the cost to 3.75 as shown for solution "b" in Fig. 5.

C. THE BALANCED 38-BUS SYSTEM

In this case, the proposed algorithm will be applied to a radial 38-bus feeder in Fig. 6. The generated Pareto Front is shown in Fig. 7. This system is different than the previous two systems as it presents a radial distribution feeder.

As expected, placing monitoring devices on the meshed system has much more significance in the overall observability compared to radial systems. This can be observed in the requirement for 100% observability, which requires 13 monitoring devices compared to only 10 in the 30-bus meshed system case. As shown from the locations of the 13 monitoring devices, all the system buses are either having a monitoring device or connected to a bus with a monitoring device. The analysis confirms that for radial feeders, to achieve 100% observability, we need to install a monitoring device on almost one third of the buses.

As shown in Fig. 6, 5 devices can achieve 42.86% loss of observability by allocating these devices on buses {2, 3, 6, 9, 12}, which are mostly the buses with lateral connections. Those buses introduce more states to be observed. Note that installing more devices have less significance on enhancing the observability. For example, installing another 5 devices, i.e. a total of 10, only reduces the loss of observability from 42.86% to 23.21% compared to the first 5 devices, which reduced the loss of observability from 100 % to 42.86 %.

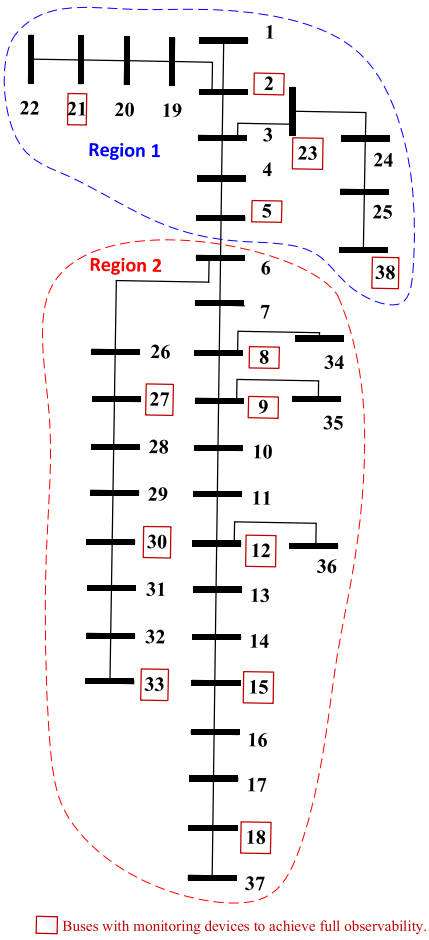

FIGURE 6. The 38-bus system [20].

Due to the fact that distribution systems serve different types of customers, e.g. commercial, industrial, residential, and agriculture, and also due to the importance of some system states to be monitored, the grid operator may assign different weights to the system states regarding their observability. To illustrate the idea, assume that the system states are divided into n subsets. In this example, assume $n = 2$; therefore, the system states are divided into two subsets: $\mathbb{S}_1 \subset \mathbb{S}$ and $\mathbb{S}_2 \subset \mathbb{S}$, where $\mathbb{S}_1 \cup \mathbb{S}_2 = \mathbb{S} = \{1, \ldots, M\}$ and $s \in \mathbb{S}$. In this example, the subsets $\mathbb{S}_1$ and $\mathbb{S}_2$ represent the states to be observed in region 1 and region 2, respectively, as shown in Fig. 6. In this case, the second objective representing the loss of the observability in the allocation problem in (9) is modified as follows:

First, we define the loss of observability γ_k of each region k, as in (10), where $k \in \mathbb{K} = \{1, 2\}$, $\mathbb{K}$ is the set of regions, and M_k is the number of states in subset $\mathbb{S}_k$. Then, the loss of observability objective can be defined as in (11). Note that if the weights ω_k for the observability of each region are the same, then the definition of f_2 in (10-11) is the same as in (9).

$$\gamma_k = \left(1 - \frac{\sum_{s \in \mathbb{S}_k} O(s)}{M_k}\right) \times 100\% \tag{10}$$

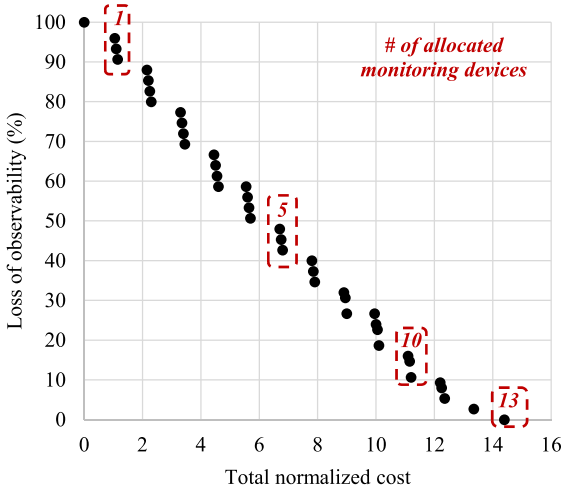

FIGURE 7. The Pareto front results for the 38-bus system.

$$f_2 = \frac{\left(\sum_k \omega_k \times M_k \times \gamma_k\right)}{\left(\sum_k \omega_k \times M_k\right)} \tag{11}$$

Therefore, the problem can be redefined as in (12).

$$\left.\begin{aligned} &\min_{X} (f_1, f_2) \\ &f_1 = \sum_{i=1}^{N} C_i \times x_i \\ &S.T.\ (4, 5, 10, 11) \\ &x_i \in \{0, 1\} \quad \forall x_i \in X \end{aligned}\right\} \tag{12}$$

For this example, assume the weights for the two regions to be $\omega_1 = 2$ and $\omega_2 = 1$. The results of the Pareto Front are shown in Fig. 8. The vertical changes in Fig. 8 represent the reallocation of the same number of devices on other buses to achieve better observability. As shown, still to achieve 0% loss of observability, 13 monitoring devices have to be installed, similar to Fig. 7. However, to achieve almost 20% loss of observability, 6 monitoring devices are required to be installed at buses $\{2, 3, 6, 9, 21, 25\}$, from which four devices are in region 1 and two devices are in region 2. The loss of observability factors in each region for this solution are $\gamma_1 = 0\%$, while $\gamma_2 = 75\%$. Thus, due to the introduced weights, the proposed approach allocated the monitoring devices to achieve 100% observability in the region with the higher weight. Fig. 8, shows the loss of observability in region 1 and 2 with the number of allocated devices. As shown in the figure, allocating 10 devices or more can result in 100% observability or 0% loss of observability in region 1. Due to the introduced weights, the proposed approach tends always to favor region 1 over region 2.

Another possible requirement from the grid operator is to ensure 100% observability for a certain region in the system. This can be performed by adding constraints to the MINLP in (9) that ensure $\gamma_k = 0\%$ for the desired regions. Therefore, the allocation problem can be defined as in (13), where $\mathbb{K}_{full} \subset \mathbb{K}$ is the subset of the desired regions with full

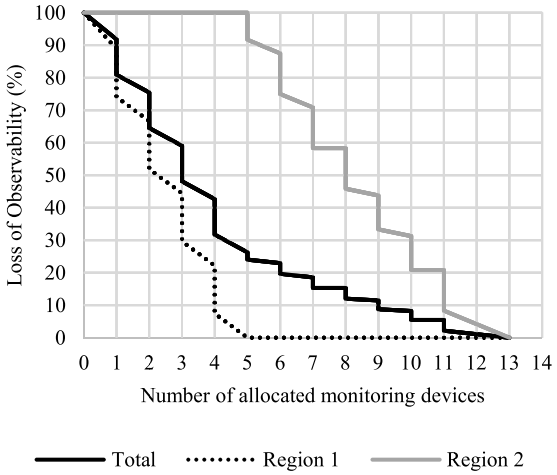

FIGURE 8. Weighted regions loss of observability for the 38-bus system.

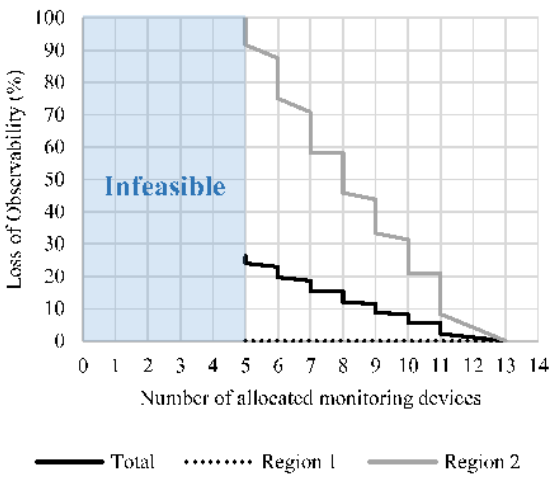

FIGURE 9. Priority regions loss of observability for the 38-bus system.

observability.

$$\left.\begin{aligned} &\min_{X} (f_1, f_2) \\ &f_1 = \sum_{i=1}^{N} C_i \times x_i \\ &f_2 = \frac{(\sum_k M_k \times \gamma_k)}{(\sum_k M_k)} \\ &\gamma_k = 0\% \quad \forall k \in \mathbb{K}_{full} \\ &S.T.\,(4, 5, 10) \\ &x_i \in \{0, 1\} \quad \forall x_i \in X \end{aligned}\right\} \tag{13}$$

For example, assume it is desired to achieve $\gamma_1 = 0\%$, while minimizing both the cost and the loss of observability in region 2, i.e. γ_2. The Pareto Front results are shown in Fig. 9. As shown, to achieve full observability in region 1, at least 5 monitoring devices are needed to be installed; thus, the region to the left of the 5 monitoring devices is infeasible. All the shown solutions achieve full observability in region 1; thus, all region 1 buses are having monitoring devices or connected to buses with monitoring devices. For example, the first allocation to achieve full observability for region 1 is performed by allocating monitoring devices on buses {2, 5, 21, 23, 38}. Another better allocation is {2, 3, 6, 21, 25, 38}, which also achieve full observability for region 1. However, the second solution has 1 device in region 2, which achieves 91.7 % loss of observability in region 2.

D. THE UNBALANCED 123-BUS SYSTEM

Finally, we test the proposed algorithm with a large-scale unbalanced 3 phase distribution system represented by the IEEE 123-bus test feeder shown in Fig. 10. All the states have the same weights in this case study, i.e. the results are based on (9). As shown in Fig. 10, the total number of monitoring devices to achieve full observability is 46 devices, which are located such that each bus has a monitoring device or connected to a monitoring device. The Pareto Front generated by the algorithm is shown in Fig. 11. Intuitively, the Pareto front is even more densely populated than the previous two cases due to the large number of decision variables present in the problem formulation. Having said that, there is an additional reason behind the increased density as well as the close proximity of the solution points. The formulation of the unbalanced system differs from the balanced one by considering the voltages and currents of each single phase of each bus as a separate state on its own. Thus, there is an increased variability in the observability loss resulting from moving the installation of a monitoring device from one bus to another, and hence a larger number of solution points.

As shown in Fig. 11, only 5 monitoring devices can reduce the loss of observability to 65%. However, as the number of allocated device increases, the significance in reducing the loss of observability decreases rapidly. For example, increasing the number of monitoring devices from 25 to 30 reduces the loss of observability from 9.4% to 5.4%. Given the large number of buses in the system, only 19 monitoring devices are needed to limit the loss of observability to below 20%.

The same allocation problem for the IEEE 123-bus system was solved using the NDSGA-II developed in [22], which converged after nearly 1000 iterations with 53 allocated monitoring devices, as shown in Fig. 12. Thus, the NDSGA-II requires 15.2% more monitoring devices to achieve full observability compared to the BARON, which only requires 46 monitoring devices as shown in Fig. 11. By comparing Fig. 11 and Fig. 12, the results show the superiority of the exact solver in achieving better observability for any number of allocated monitoring devices.

As discussed earlier, the set of solutions presented by the Pareto Front are all equally optimal in the sense that no other solution can be found that can further improve the collective values of the objective functions. However, the final compromise solution to be selected is based on the desired trade-off between cost and observability and the operational preferences of the planning entity. A popular method for selecting a compromising solution from the Pareto optimal set is based on minimizing the distance between the Pareto Front and the ideal solution point [23].

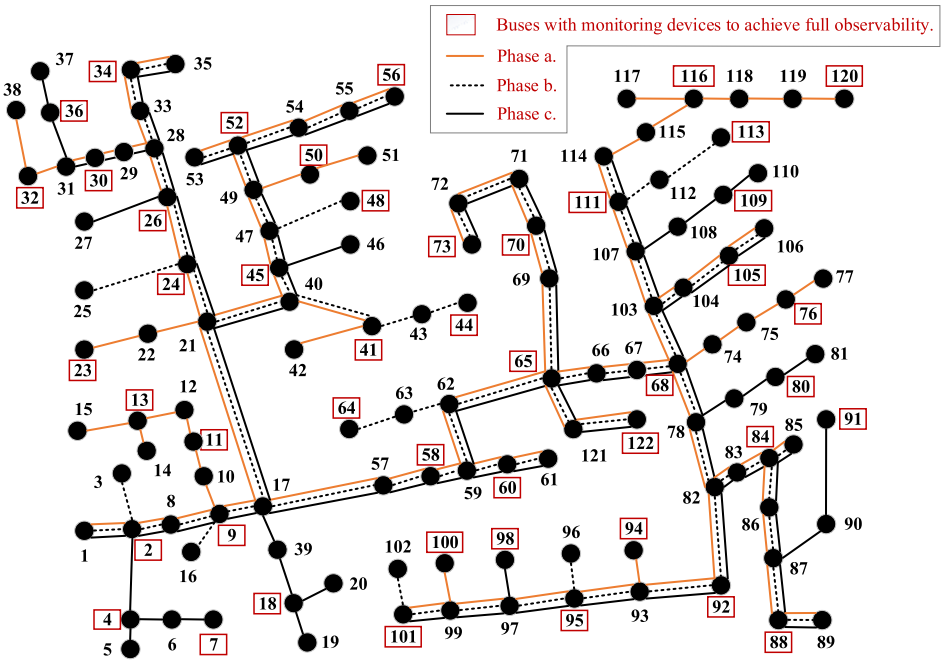

FIGURE 10. The IEEE 123-bus test feeder [21].

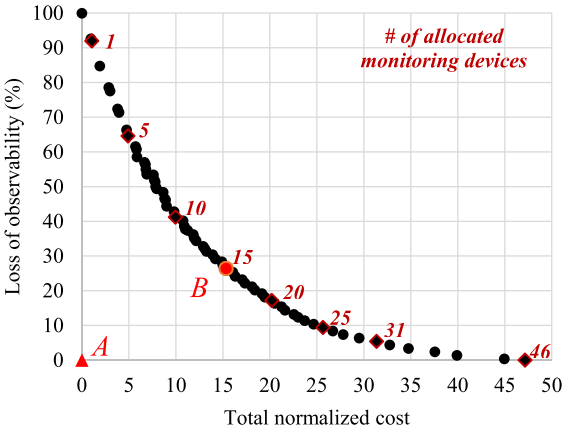

FIGURE 11. The Pareto front for the IEEE 123-bus test feeder.

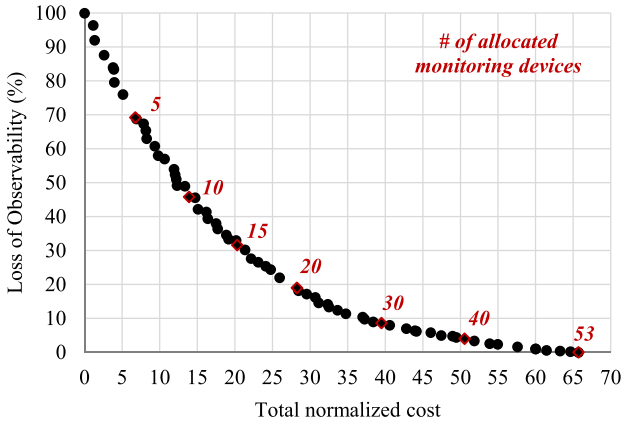

FIGURE 12. The Pareto front for the IEEE 123-bus test feeder using the NDSGA.

The origin point A in Fig. 11 corresponding to 0 cost and 0% loss of observability, presents the ideal case in this scenario as it theoretically minimizes both objective functions. However, this point is practically infeasible and hence, the compromising optimal solution can be found by finding the closest point from the Pareto Front to that point. More concretely, we can employ a metric that indicates the dissatisfaction associated with choosing an optimal solution as our selecting criteria [23]. Define the dissatisfaction $z_{u,q}$ of any solution x_u on the Pareto Front with respect to objective f_q as

$$z_{u,q} = \frac{f_q(x_u) - f_q^{MIN}}{f_q^{MAX} - f_q^{MIN}}, \tag{14}$$

where $u \in \{1, 2, \ldots, U\}$ is the index of Pareto Front solutions, U is the number of Pareto Front solutions, $q \in \{1, 2, \ldots, Q\}$ is the index of objective functions, Q is the number of objective functions, which is 2 in our case, $f_q(x_u)$ is the value of objective q corresponding to solution x_u, f_q^{MIN} and f_q^{MAX} are the maximum and minimum values for objective q. In this case study, the minimum and maximum values are as follows: $f_1^{MIN} = 0, f_1^{MAX} = 47.15, f_2^{MIN} = 0$, and $f_2^{MAX} = 100$.

To find a compromise solution among $U = 71$ solutions, we minimize the dissatisfaction or the distance of each solution to the ideal point, viz.

$$\min_u \left(\sqrt{\sum_{q=1}^{Q} z_{u,q}^2} \right) \tag{15}$$

The best compromise solution is thus found to be point B indicated in Fig. 11 as it represents the closest point

Algorithm 1 Connectivity and Co-Connectivity Parameters Generation for Unbalanced Systems

Read line segment data
Construct Connection Parameter $D^{UNB}_{l,k,p}$
Calculate M^V, M^I, and M as in (3)
procedure GENERATE A
  Initialize $A = [0]_{M\times N}$
  $s = 1$
  for each integer i in $1 : N$ **do**
    for each integer p in $1 : 3$ **do**
      $j = i$
      if $D^{UNB}_{i,j,p} == 1$ **then**
        $A_{s,i} = 1$
      end if
      Increment s
    end for
  end for
  $s = M^V + 1$
  for each integer i in $1 : N$ **do**
    for each integer j in $i + 1 : N$ **do**
      for each integer p in $1 : 3$ **do**
        if $D^{UNB}_{i,j,p} == 1$ **then**
          $A(s, i) = 1, A(s, j) = 1$
          Increment s
        end if
      end for
    end for
  end for
end procedure
procedure GENERATE B^{CC1}, B^{CC2}
  Initialize $B^{CC1} = [0]_{M\times N}$, $B^{CC2} = [0]_{M\times N}$
  $s = M^V + 1$
  for each integer i in $1 : N$ **do**
    for each integer j in $i + 1 : N$ **do**
      for each integer p in $1 : 3$ **do**
        if $D^{UNB}_{i,j,p} == 1$ **then**
          $B^{CC1}(s, :) = A(i, :)$
          $B^{CC2}(s, :) = A(j, :)$
          Increment s
        end if
      end for
    end for
  end for
end procedure

to the ideal point $\{f_1^{MIN}, f_2^{MIN}\} = \{0, 0\}$. The solution is represented by point B in Fig. 11, which corresponds to a normalized cost of 26.4 and an observability loss of 15.35% with 15 monitoring devices installed.

VIII. CONCLUSION

An optimal monitoring devices allocation algorithm is of the utmost importance for any distribution system planning process. Achieving the right tradeoff between cost and observability might be the critical factor that would allow any distribution system to deliver high quality service given its limited budget. In this paper, we explored generating the set of Pareto optimal solutions that would illustrate the tradeoff between cost and observability. Formulating the problem as a multi-objective optimization problem with the aim of simultaneously reducing the cost and the loss of observability in the system, we use a branch-and-reduce based algorithm to generate the set of true Pareto optimal solutions and enable the cost-benefit analysis of multiple, equally optimal solutions. Simulation results prove that the proposed algorithm is effective for both three-phase balanced and unbalanced distribution systems.

APPENDIX A

See Algorithm 1.

REFERENCES

[1] O. Samuelsson, M. Hemmingsson, A. H. Nielsen, K. O. H. Pedersen, and J. Rasmussen, "Monitoring of power system events at transmission and distribution level," *IEEE Trans. Power Syst.*, vol. 21, no. 2, pp. 1007–1008, May 2006.

[2] P. E. T. Martins, M. Oleskovicz, A. L. da Silva Pessoa, and I. de Moura Faria, "Optimized allocation of power quality monitors in distribution systems considering fault location," in *Proc. 18th Int. Conf. Harmon. Qual. Power (ICHQP)*, Ljubljana, Slovenia, May 2018, pp. 1–6.

[3] N. M. Manousakis, G. N. Korres, and P. S. Georgilakis, "Taxonomy of PMU placement methodologies," *IEEE Trans. Power Syst.*, vol. 27, no. 2, pp. 1070–1077, May 2012.

[4] A. F. de Freitas, F. V. Amaral, J. A. L. Silva, R. R. Saldanha, and S. M. Silva, "Optimum allocation of power quality monitors in electric power systems—A case study," in *Proc. 17th Int. Conf. Harmon. Qual. Power (ICHQP)*, Belo Horizonte, Brazil, Oct. 2016, pp. 768–773.

[5] P. E. T. Martins, W. G. Zvietcovich, T. A. de Oliveira Silva, and B. J. de Jesus, "Allocation of power quality monitors by Clonal algorithm," in *Proc. 17th Int. Conf. Harmon. Qual. Power (ICHQP)*, Belo Horizonte, Brazil, Oct. 2016, pp. 980–985.

[6] L. G. de O. Silva, A. A. P. da Silva, and A. T. de Almeida-Filho, "Allocation of power-quality monitors using the P-median to identify nontechnical losses," *IEEE Trans. Power Del.*, vol. 31, no. 5, pp. 2242–2249, Oct. 2016.

[7] M. Oleskovicz, H. M. G. C. Branco, R. P. M. da Silva, D. V. Coury, and A. C. B. Delbem, "A compact genetic algorithm structure used for the optimum allocation of power quality monitors based on electrical circuit topology," in *Proc. IEEE 15th Int. Conf. Harmon. Qual. Power*, Hong Kong, Jun. 2012, pp. 34–39.

[8] H. M. G. C. Branco, R. P. M. da Silva, M. Oleskovicz, D. V. Coury, and A. C. B. Delbem, "Extended compact genetic algorithm applied for optimum allocation of power quality monitors in transmission systems," in *Proc. IEEE Power Energy Soc. Gen. Meeting*, San Diego, CA, USA, Jul. 2011, pp. 1–6.

[9] J. C. Cebrian, C. F. M. Almeida, and N. Kagan, "Genetic algorithms applied for the optimal allocation of power quality monitors in distribution networks," in *Proc. 14th Int. Conf. Harmon. Qual. Power-(ICHQP)* Bergamo, Italy, Sep. 2010, pp. 1–10.

[10] C. F. M. Almeida and N. Kagan, "Allocation of power quality monitors by genetic algorithms and fuzzy sets theory," in *Proc. 15th Int. Conf. Intell. Syst. Appl. Power Syst.*, Curitiba, Brazil, Nov. 2009, pp. 1–6.

[11] D. C. S. Reis, P. R. C. Villela, C. A. Duque, and P. F. Ribeiro, "Transmission systems power quality monitors allocation," in *Proc. 21st Century IEEE Power Energy Soc. Gen. Meeting-Convers. Del. Elect. Energy*, Pittsburgh, PA, USA, Jul. 2008, pp. 1–7.

[12] T. R. Kempner, M. Oleskovicz, and A. Q. Santos, "Optimal allocation of monitors by analyzing the vulnerability area against voltage sags," in *Proc. 16th Int. Conf. Harmon. Qual. Power (ICHQP)*, Bucharest, Romania, May 2014, pp. 536–540.

[13] X. Dai, H. Yang, and W. Cai, "An optimum allocation method of power quality monitors by considering voltage dip," in *Proc. Asia-Pacific Power Energy Eng. Conf.*, Wuhan, China, Mar. 2011, pp. 1–4.

[14] M. A. Eldery, E. F. El-Saadany, M. M. A. Salama, and A. Vannelli, "A novel power quality monitoring allocation algorithm," *IEEE Trans. Power Del.*, vol. 21, no. 2, pp. 768–777, Apr. 2006.
[15] C. Peng, H. Sun, and J. Guo, "Multi-objective optimal PMU placement using a non-dominated sorting differential evolution algorithm," *Int. J. Elect. Power Energy Syst.*, vol. 32, no. 8, pp. 886–892, Oct. 2010.
[16] M. F. Shaaban and E. F. El-Saadany, "Accommodating high penetrations of PEVs and renewable DG considering uncertainties in distribution systems," *IEEE Trans. Power Syst.*, vol. 29, no. 1, pp. 259–270, Jan. 2014.
[17] G. Liu, Y. L. Zhu, and W. Jiang, "Wind-thermal dynamic economic emission dispatch with a hybrid multi-objective algorithm based on wind speed statistical analysis," *IET Gener., Transmiss. Distrib.*, vol. 12, no. 17, pp. 3972–3984, Sep. 2018.
[18] H. R. Baghaee, M. Mirsalim, G. B. Gharehpetian, and H. A. Talebi, "MOPSO/FDMT-based Pareto-optimal solution for coordination of overcurrent relays in interconnected networks and multi-DER microgrids," *IET Gener., Transmiss. Distrib.*, vol. 12, no. 12, pp. 2871–2886, Jul. 2018.
[19] N. Sahinidis. (2015). BARON Solver Manual. GAMS Development Corporation, Washington, DC, USA. Accessed: Feb. 20, 2019. [Online]. Available: https://www.gams.com/latest/docs/S_BARON.html
[20] D. Singh, R. K. Misra, and D. Singh, "Effect of load models in distributed generation planning," *IEEE Trans. Power Syst.*, vol. 22, no. 4, pp. 2204–2212, Nov. 2007.
[21] *IEEE 123 Node Test Feeder*. Accessed Feb. 20, 2019. [Online]. Available: http://sites.ieee.org/pes-testfeeders/resources/
[22] K. Deb, A. Pratap, S. Agarwal, and T. Meyarivan, "A fast and elitist multiobjective genetic algorithm: NSGA-II," *IEEE Trans. Evol. Comput.*, vol. 6, no. 2, pp. 182–197, Apr. 2002.
[23] H. Eschenauer, J. Koski, and E. Osyczka, Eds., *Multicriteria Design Optimization: Procedures and Applications*. Berlin, Germany: Springer-Verlag, 1990.

MOSTAFA F. SHAABAN (S'11–M'15) received the B.Sc. and M.Sc. degrees in electrical engineering from Ain Shams University, Cairo, Egypt, in 2004 and 2008, respectively, and the Ph.D. degree in electrical engineering from the University of Waterloo, Waterloo, ON, Canada, in 2014.

He is currently an Assistant Professor with the Department of Electrical Engineering, American University of Sharjah, Sharjah, UAE. His research interests include smart grid, renewable DG, distribution system planning, electric vehicles, storage systems, and bulk power system reliability.

AHMED H. OSMAN received the B.Sc. and M.Sc. degrees in electrical engineering from Helwan University, Cairo, Egypt, in 1991 and 1996, respectively, and the Ph.D. degree in electrical engineering from the University of Calgary, Calgary, AB, Canada, in 2003. From 2004 to 2008, he was an Assistant Professor with the Department of Electrical and Computer Engineering, University of Calgary. He is currently an Associate Professor with the Department of Electrical Engineering, American University of Sharjah, Sharjah, UAE. His research interests and activities include power system analysis and power system protection.

FATEMA M. ASEERI received the B.Sc. and M.Sc. degrees in electrical engineering from the American University of Sharjah, Sharjah, UAE, in 2015 and 2017, respectively. From 2017 to 2018, she was a Research Assistant with the Department of Electrical Engineering, American University of Sharjah. Her research interests include wireless networking and power system monitoring.